Eur. Phys. J. D **59**, 193–200 (2010)
DOI: 10.1140/epjd/e2010-00135-3

THE EUROPEAN PHYSICAL JOURNAL D

Regular Article

Ionization of the hydrogen atom by short half-cycle pulses: dependence on the pulse duration

D.G. Arbó[1,2], M.S. Gravielle[1,2], K.I. Dimitriou[3,4,5], K. Tőkési[6,a], S. Borbély[7], and J.E. Miraglia[1,2]

[1] Institute for Astronomy and Space Physics, IAFE, CC 67, Suc. 28 (1428) Buenos Aires, Argentina
[2] Department of Physics, FCEN, University of Buenos Aires, Argentina
[3] Department of Physical Science and Applications, Hellenic Army Academy, Vari, Greece
[4] Department of Informatics, Technological Educational Institution, Lamia, Greece
[5] Institute of Theoretical and Chemical Physics, National Hellenic Research Foundation, Athens, Greece
[6] Institute of Nuclear Research of the Hungarian Academy of Science, ATOMKI, PO Box 51, 4001 Debrecen, Hungary
[7] Faculty of Physics, Babes-Bolyai University, Cluj-Napoca, Romania

Received 30 December 2009 / Received in final form 1st April 2010
Published online 12 May 2010 –

Abstract. A theoretical study of the ionization of hydrogen atoms by short external half-cycle pulses (HCPs) as a function of the pulse duration, using different quantum and classical approaches, is presented. Total ionization probability and energy distributions of ejected electrons are calculated in the framework of the singly-distorted Coulomb-Volkov (SDCV) and the doubly-distorted Coulomb-Volkov (DDCV) approximations. We also performed quasiclassical calculations based on a classical trajectory Monte Carlo method which includes the possibility of tunneling (CTMC-T). Quantum and classical results are compared to the numerical solution of the time-dependent Schrödinger equation (TDSE). We find that for high momentum transfers the DDCV shows an improvement compared to the SDCV, especially in the low-energy region of the electron emission spectra, where SDCV fails. In addition, DDCV reproduces successfully the TDSE electron energy distributions at weak momentum transfers. CTMC-T results reveal the importance of tunneling in the ionization process for relative long pulses and strong momentum transfers but fails to overcome the well-known classical suppression observed for weak electric fields.

1 Introduction

In the last decade short unidirectional electric pulses, called half-cycle pulses (HCPs), have had several applications like focusing of Rydberg wave packets, production of one-dimensional Rydberg atoms, and generation of quasi-classical Bohr-alike atoms [1,2]. The aim of this work is to investigate the applicability of several quantum distorted-wave and classical methods to describe the action of such HCP on atomic targets. Time-dependent distorted wave theory has been widely used to describe ionization processes of various atomic targets interacting with short laser pulses [3–10]. In this way, the collision dynamics due to the effects of the core potential on the released electron can be directly probed. Time-dependent distorted-wave methods gain importance in those cases where the time-dependent Schrödinger equation becomes impractical, for instance, at high intensities and long pulse durations. Atomic ionization was previously studied within the Coulomb-Volkov approximation using the velocity gauge [11] and compared to the length-gauge results [12–14]. Here, we will analyze two different distorted-wave approaches – singly-distorted Coulomb-Volkov (SDCV) and doubly-distorted Coulomb-Volkov approximations (DDCV) – which differ according to what channels are distorted. Whereas the SDCV is a single distorted method [15–20] that includes the effect of the remaining core only on the final state, in the DDCV both final and initial channels are distorted and, consequently, its computation involves two-center Coulomb integrals [16].

Besides the recent developments of quantum approximations, classical and quasi-classical approaches have also attracted considerable interest. Especially, the classical trajectory Monte Carlo (CTMC) method has been successfully applied to atomic collisions for more than forty years [21]. This method is based on the numerical integration of the classical equations of motion of the particles attending in the scattering system. For the cases of atomic collisions at intermediate energies, where the quantum mechanical calculations become very complicated or intractable, CTMC becomes a powerful tool [22,23]. However, for short electric fields interacting with atoms, quantum effects such as tunneling and multiphoton processes might become important, leading to the failure of a pure classical approach. In order to include some of the quantum effects in the classical calculation, a modification of the CTMC considering the possibility of ionization by tunneling (CTMC-T) was developed [24–26]. The CTMC-T method has been quite successful in dealing with

[a] e-mail: tokesi@atomki.hu

atomic photoionization processes when infrared electromagnetic fields are strong enough to allow tunneling ionization of the atomic target [24–27].

In our previous works [28,29] we have studied the ionization of hydrogen atoms by a sudden momentum transfer or kick, approximated by a delta function in the time domain. In the present work we extend these studies for short half-cycle pulses (HCP) of finite (non-zero) duration, where the pulse can be longer than the classical orbital period of the electron in the initial state and, therefore, the sudden approximation – when the effect of a short pulse on one atom can be treated within the framework of a sudden momentum transfer [2,30,31] – is no longer valid. We analyze the efficiency of the SDCV and the CTMC method without tunneling to describe ejected electron emission spectra following the ionization of a hydrogen atom by HCPs. The results are compared with their respective improved methods: DDCV and CTMC-T. We also analyze the effect of the time duration of the pulse on the ionization yield, determining the validity range of the sudden approximation. In addition, results of the different approximations are compared to those obtained by numerical calculations of the time dependent Schrödinger equation (TDSE).

The paper is organized as follows: in Section 2.1 we briefly describe the employed time-dependent distorted wave theories: (i) the sudden Coulomb-Volkov (SCV) approximation, (ii) the singly-distorted Coulomb-Volkov approximation (SDCV), and (iii) the doubly-distorted Coulomb-Volkov approximation (DDCV). In Section 2.2 we shortly introduce the quasiclassical trajectory Monte Carlo (CTMC-T) method where the Hamilton equations of motion of the electron are solved including the possibility of tunnel ionization. In Section 3.1 we present the results of our calculations of the total ionization probability as a function of the pulse duration. In Section 3.2 results of the energy distribution of the ejected electrons are illustrated and discussed. Finally, in Section 4 we present the conclusions of the theoretical studies developed in this paper. Atomic units are used throughout the paper.

2 Theory

The total Hamiltonian of a hydrogen atom interacting with an external electric pulse in the dipole approximation is

$$H(t) = H_0 + V(t), \tag{1}$$

where $H_0 = \mathbf{p}^2/2 - Z/r$ is the atomic Hamiltonian, Z is the atomic charge ($Z = 1$ for the case of the hydrogen atom), $\mathbf{p}$ and $\mathbf{r}$ are the momentum and position of the electron, respectively, and $V(t) = \mathbf{r}\cdot\mathbf{F}(t)$ is the interaction term with the external electric field $\mathbf{F}(t)$ in the length gauge. For convenience, we model the external electric field as

$$\mathbf{F}(t) = \begin{cases} F_0(\tau)\cos^2\left(\frac{\pi t}{\tau}\right)\cos(\omega t)\ \hat{\mathbf{z}}\,, & -\tau/2 \le t \le \tau/2 \\ \mathbf{0} & \text{elsewhere} \end{cases} \tag{2}$$

where τ is the total pulse duration, $F_0(\tau)$ is the τ-dependent peak field, and the linearly polarized electric field is along the $\hat{\mathbf{z}}$ direction. Equation (2) can describe either the electric field of a laser of carrier frequency ω when $\tau \gg \omega^{-1}$ or a half-cycle pulse (HCP) when $\tau \lesssim \omega^{-1}$. In the latter, in order to assure the total momentum transfer $\mathbf{\Delta p} = \int_{-\infty}^{+\infty} dt\ \mathbf{F}(\mathbf{t})$ to be τ-invariant, we must use the following expression for the peak field,

$$F_0(\tau) = \frac{-\omega\Delta p}{\sin(\omega\tau/2)}\left(1 - \frac{\omega^2\tau^2}{4\pi^2}\right). \tag{3}$$

The minus sign stems from the electron charge and $\Delta p = |\mathbf{\Delta p}|$. In the sudden limit, i.e., $\tau \to 0$, the field becomes a sudden momentum transfer or "kick", i.e., $\mathbf{F}(t) = -\mathbf{\Delta p}\,\delta(t)$ (see Eq. (3)).

Our study is confined to a hydrogen atom initially in its ground state subject to a short HCP, i.e., $\tau \lesssim \pi\omega^{-1}$. We calculate the ionization yield by solving the quantum and classical equations of motion as explained in the next sections.

2.1 Time-dependent distorted-wave theories

The electron, initially bound to the atomic nucleus in the state $|\phi_i\rangle$ with energy ε_i, is emitted with momentum $\mathbf{k}$ and energy $E = k^2/2$ due to the interaction with the external field $\mathbf{F}(t)$, ending in the final state $\phi^-_{\mathbf{k}}$. Energy distributions of ejected electrons can be calculated from the transition matrix as

$$\frac{dP}{dE} = \sqrt{2E}\int d\Omega\ \left|T_{if}\right|^2, \tag{4}$$

where T_{if} is the T-matrix element corresponding to the transition $\phi_i \to \phi^-_{\mathbf{k}}$ and Ω is the solid angle of the electron momentum $\mathbf{k}$.

Here we evaluate the transition matrix within the framework of the time-dependent distorted-wave theory by using different Coulomb-Volkov-type approximations: the SCV, the SDCV, and the DDCV. All of them use the usual Coulomb-Volkov distorted-wave function $\chi_f^{CV-}(t)$ to represent the final channel. It reads as [18,19]

$$\chi_f^{\mathrm{CV}-}(\mathbf{r},t) = \phi^-_{\mathbf{k}}(\mathbf{r},t)\exp(iD^-(\mathbf{k},\mathbf{r},t)), \tag{5}$$

where $\phi^-_{\mathbf{k}}$ is the unperturbed final state given by

$$\phi^-_{\mathbf{k}}(\mathbf{r},t) = \mathrm{e}^{-i\frac{k^2}{2}t}\frac{\exp(i\mathbf{k}\cdot\mathbf{r})}{(2\pi)^{3/2}}\ \mathcal{D}_C(Z,\mathbf{k},\mathbf{r}), \tag{6}$$

and $\mathcal{D}_C(Z,\mathbf{k},\mathbf{r}) = N_T^-(k)\ {}_1F_1(-iZ/k, 1, -ik\,r - i\mathbf{k}\cdot\mathbf{r})$ is the Coulomb distortion factor, with $N_T^-(k) = \exp(\pi Z/2k)\,\Gamma(1 + iZ/k)$ and ${}_1F_1$ the confluent hypergeometric function. The Volkov phase D^- in equation (5) is given by [32]

$$D^{\pm}(\mathbf{k},\mathbf{r},t) = \mathbf{A}^{\pm}(t)\cdot\mathbf{r} - \mathbf{k}\cdot\alpha^{\pm}(t) - \beta^{\pm}(t), \tag{7}$$

where $\mathbf{A}^{\pm}(t) = -\int_{\mp\infty}^{t} dt' \ \mathbf{F}(t')$ is the vector potential divided by the speed of light, $\alpha^{\pm}(t) = \int_{\mp\infty}^{t} dt' \mathbf{A}^{\pm}(t')$ represents the classical displacement of the free electron from the atomic nucleus, and $\beta^{\pm}(t) = \frac{1}{2}\int_{\mp\infty}^{t} dt' \ (\mathbf{A}^{\pm}(t'))^2$ is related to the ponderomotive shift of the energy.

Transition matrix derived from the different distorted-wave methods are summarized below.

(i) Sudden Coulomb-Volkov approximation:
In the *prior* form SCV T-matrix element is expressed as [16,18,19]

$$T_{if}^{\mathrm{SCV}} = \lim_{t\to-\tau/2} \langle \chi_f^{\mathrm{CV}-}(t) \, | \phi_i(t) \rangle \, , \tag{8}$$

where $|\phi_i(t)\rangle = |\phi_i\rangle \exp(-i\varepsilon_i t)$ is the initial unperturbed state.
In particular, when the external field is reduced to a sudden momentum transfer of strength $\mathbf{\Delta p}$, i.e., $\lim_{\tau\to 0} \mathbf{F}(t) = -\mathbf{\Delta p} \ \delta(t)$, the absolute value of the SCV transition matrix for HCPs becomes [28,29]

$$|T_{if}^{\mathrm{SCV}}| = \left| \langle \phi_{\mathbf{k}}^{-} | \, e^{i\mathbf{\Delta p}\cdot\mathbf{r}} \ |\phi_i(-\tau/2)\rangle \right| , \tag{9}$$

which coincides with the exact quantum transition matrix in the sudden limit. Hence, the SCV reckons the interaction between the electron and the external field of finite duration as a sudden momentum transfer, being strictly valid as $\tau \to 0$ [28,29].

(ii) Singly-distorted Coulomb-Volkov approximation:
The *post* form of the transition amplitude within the SDCV is given by [16]

$$T_{if}^{\mathrm{SDCV}} = -i \int_{-\tau/2}^{\tau/2} dt \ \langle \chi_f^{\mathrm{CV}-}(t) | V(t) \, | \phi_i(t) \rangle \, . \tag{10}$$

Again, it reduces to equation (9) for sudden momentum transfers [28,29].

(iii) Doubly-distorted Coulomb-Volkov approximation:
In the DDCV the transition amplitude is evaluated by distorting both initial and final states on equal footing. It reads [16]

$$T_{if}^{\mathrm{DDCV}} = T_{if}^{\mathrm{SCV}} - i \int_{-\tau/2}^{\tau/2} dt \ \langle \chi_f^{\mathrm{CV}-}(t) | W_f^{\dagger} \, | \chi_i^{\mathrm{CV}+}(t) \rangle \, , \tag{11}$$

where T_{if}^{SCV} is the transition amplitude in the SCV approximation given in equation (8) and the initial Coulomb-Volkov distorted wave function $\chi_i^{\mathrm{CV}+}(t)$ is expressed as [16]

$$\chi_i^{\mathrm{CV}+}(\mathbf{r},t) = \phi_i[\mathbf{r} - \alpha^{+}(t)] \mathrm{e}^{iD^{+}(\mathbf{0},\mathbf{r},t)} \mathrm{e}^{-i\varepsilon_i t}. \tag{12}$$

In equation (11) the operator $W_f(t)$ acts on the final distorted state in the following way

$$W_f \chi_f^{\mathrm{CV}-}(\mathbf{r},t) = -i \, [\nabla - i\mathbf{k}] \, \phi_{\mathbf{k}}^{-}(\mathbf{r},t) \cdot \mathbf{A}^{-}(t) \times \exp[iD^{-}(\mathbf{k},\mathbf{r},t)]. \tag{13}$$

Notice that previous calculations of the time-dependent doubly distorted-wave transition probabilities [16] neglect the term $\alpha^{+}(t)$ in the argument of ϕ_i of equation (12). It is a reasonable approximation when the classical electron maximum displacement α_0 is smaller than the Bohr radius, i.e., $\alpha_0 < 1$. Unfortunately, this is not the case for most of the experiments and, therefore, the consideration of $\alpha^{+}(t)$ into equation (12) leads to two-center Coulomb integrals which need to be solved numerically. For a short HCP the maximum displacement occurs at the end of the perturbation, i.e., $t = \tau/2$, and can be estimated as $\alpha_0 = \alpha^{+}(\tau/2) \simeq \tau\Delta p$, which is strictly valid in the sudden limit. It can be easily seen that the DDCV transition amplitude also collapses to the SCV in the limit of sudden momentum transfers [28,29], i.e., $\lim_{\tau\to 0} T_{if}^{\mathrm{DDCV}} = T_{if}^{\mathrm{SCV}}$, since the second term of equation (11) goes to zero as $\tau \to 0$.

2.2 Quasiclassical simulation

The classical trajectory Monte Carlo method (CTMC) is a non-perturbative method where classical equations of motion are solved numerically. The microcanonical ensemble that characterizes the initial state of the target is assumed to be

$$\rho_{\varepsilon_i}(\mathbf{r},\mathbf{p}) = C_1 \delta(\varepsilon_i - E) = C_1 \delta\left(\varepsilon_i - \frac{1}{2}\mathbf{p}^2 + \frac{Z}{r}\right), \tag{14}$$

where C_1 is a normalization constant and ε_i is the binding energy of the active electron. In the present CTMC approach, Hamilton's classical nonrelativistic equations of motion are solved numerically for a large set of electron initial conditions [22,33,34]. We include the tunnel effect in the classical method (CTMC-T) by allowing the electron to pass through the potential barrier whenever certain conditions are satisfied [24–26], namely each time the electron reaches the outer turning point, where $p_z = 0$ and $z\,F(t) < 0$, the tunneling probability is calculated according to the WKB approximation [35–37]. At that time, the trajectory bifurcates: it either tunnels through the potential barrier or continues inside the potential barrier. This procedure is repeated each time the electron encounters the outer turning point until the end of the pulse for a given set of the electron initial conditions [38]. We note that since the WKB formula is strictly valid for one-dimensional systems, application to the 3D system requires the choice of an appropriate tunneling path. For the calculation of the tunneling probability, we choose the path across the potential barrier which ends up on the same energy manifold and maximizes the tunneling probability [24–26]. Tunneling of the electron from the continuum back to the interior of the Coulomb well has a negligible probability [24,25] and it is therefore not included in the present model.

For the ionization channel the final energy of the ejected electron was recorded. The differential ionization probability (P_i) was computed with the following formula:

$$P_i = \frac{dP}{dE} = \frac{N_i}{N\Delta E}, \tag{15}$$

where N is the total number of classical trajectories calculated for the given collision system, N_i is the number of trajectories that satisfy the criteria for ionization under consideration in the energy interval (or box dimension) ΔE of the electron. Equation (15) is directly applicable in the CTMC calculations. However, in the CTMC-T calculations the number of trajectories N_i has to be properly weighted according to the bifurcation procedure. The standard deviation for a differential probability is defined through

$$\Delta P_i = P_i \left[\frac{N - N_i}{N N_i} \right]^{1/2}. \tag{16}$$

2.3 TDSE calculations

The time-dependent Schrödinger equation is solved by means of the generalized pseudo-spectral method [39]. Briefly, the method combines a discretization of the radial coordinate optimized for the Coulomb singularity with quadrature methods to achieve stable long-time evolution using a split-operator method. It allows for an accurate description of both the unbound as well as the bound parts of the total wave function $|\psi(t)\rangle$. Details of the calculations can be found for example in references [39,40]. The process of detecting an electron of momentum $\mathbf{k}$ can then be viewed as a projection of the wave function onto the Coulomb waves after the laser pulse is turned off [41–43]. Therefore, the energy distributions are obtained as

$$\frac{dP}{dE} = \sum_l |\langle k, l \,|\psi(\tau)\rangle|^2 , \tag{17}$$

where $|k, l\rangle$ is the eigenstate of the free atomic Hamiltonian with positive eigenenergy $E = k^2/2$ and orbital quantum number l. Cylindrical symmetry reduces the dynamics into a two-dimensional problem. The projection of the angular momentum on the polarization direction of the laser is a constant of motion (the magnetic quantum number m is unaffected during the time evolution). As the initial state of the system we consider the ground state of the hydrogen atom, i.e. $m = 0$. The numerical solution of the time-dependent Schrödinger equation can be considered as exact because it does not have any physical approximation, i.e., errors are only of numerical nature. This is the reason why we use it as benchmark for assessing the reliability of the quasiclassical (CTMC-T) and quantum (DDCV, SDCV) approximations described above.

3 Results and discussion

3.1 Total ionization probability

The total ionization probability was derived from energy distributions by integrating over all positive energies, i.e. $P_{\rm ion} = \int_0^\infty dE\ (dP/dE)$. It is known that at high momentum transfers, i.e., $\Delta p \gg 1$ a.u., both classical and quantum mechanics predict almost full ionization in the sudden limit ($\tau \to 0$) [28,29]. For example, for $\Delta p = 2.5$ a.u. the total classical ionization probability is 96.1%, while the quantum one is 96.8%. Hereafter, we intend to reveal how the total ionization probability depends on the duration of the HCP and the strength of the momentum transfer. In all our calculations we have used HCPs with an electric field given by equation (2) with $\omega = 0.05$ a.u. and a τ-dependent peak field F_0 given by equation (3). Similar HCPs occur during the ionization of atomic systems by charged particle impact [44,45].

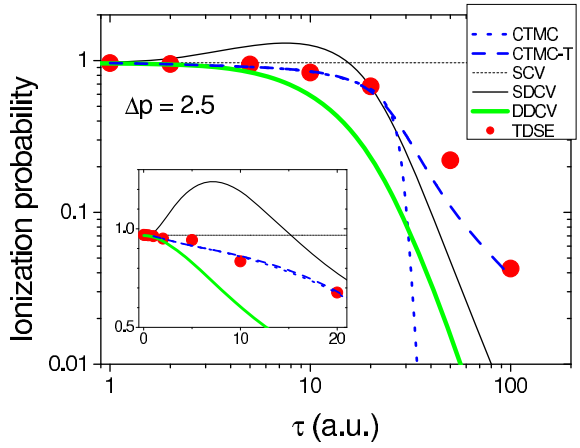

Fig. 1. (Color online) Total ionization probability as a function of the pulse duration after a pulse of momentum transfer $\Delta p = 2.5$ a.u. Dotted (blue) line: CTMC, dashed (blue) line: CTMC-T, thin short-dashed line: SCV, thin black solid line: SDCV, and (green) gray thick solid line: DDCV. (Red) dots correspond to TDSE calculations.

In Figure 1, the total ionization probability $P_{\rm ion}$ is displayed for $\Delta p = 2.5$ a.u. as a function of the pulse duration. Quantum SDCV and DDCV results converge to the sudden limit as $\tau \to 0$, which is a necessary condition for a good quantum approximation. But SDCV grows reaching a maximum value and then starts a steep fall as τ increases. This anomalous behavior of the SDCV leads to absurd results, i.e., $P_{\rm ion} > 1$ in a wide range of pulse durations: $2 \lesssim \tau \lesssim 15$ a.u. This deficiency of the SDCV is solved by the DDCV, which exhibits a monotonically decreasing ionization probability as a function of the pulse duration. Nevertheless, DDCV underestimates the total ionization probability for more than one order of magnitude for very long pulses, compared with the numerical results of TDSE. The fail of the SDCV and DDCV is due to the fact that both approaches are based on perturbative theories and, therefore, they are not expected to work properly when $\Delta p \gg 1$ a.u. On the other side, CTMC and CTMC-T are not perturbative approaches in the sense that the external field of the HCP and the Coulomb interaction are fully taken into account. This is the reason why the most accurate approximation for long pulses $\tau > 30$ a.u. and high momentum transfers $\Delta p = 2.5$ a.u., is the quasiclassical CTMC-T approach.

The essential agreement between classical and quantum results in the sudden limit can be also observed for very short pulses, i.e., $\tau \lesssim 2$ a.u. Both CTMC and

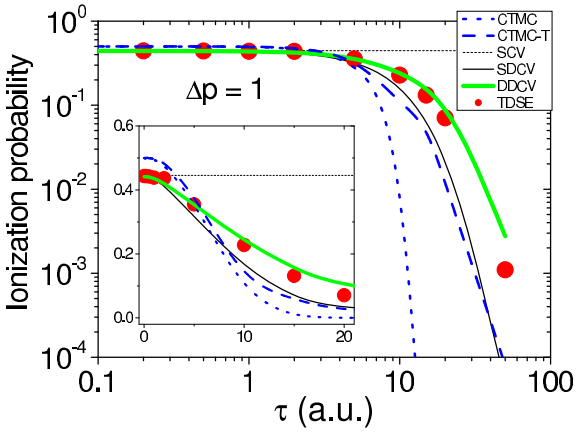

Fig. 2. (Color online) Total ionization probability as a function of the pulse duration after a pulse of momentum transfer $\Delta p = 1$ a.u. Dotted (blue) line: CTMC, dashed (blue) line: CTMC-T, thin short-dashed line: SCV, thin black solid line: SDCV, and (green) gray thick solid line: DDCV. (Red) dots correspond to TDSE calculations.

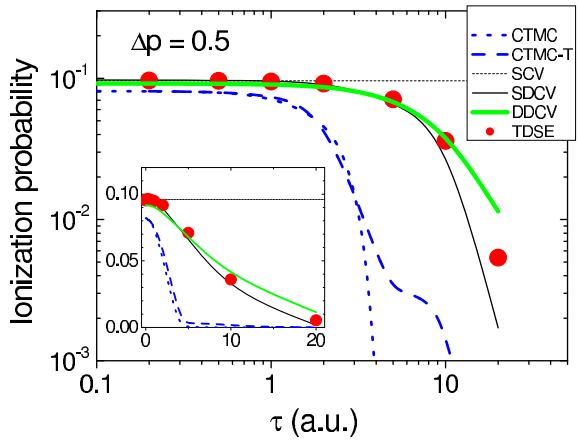

Fig. 3. (Color online) Total ionization probability as a function of the pulse duration after a pulse of momentum transfer $\Delta p = 0.5$ a.u. Dotted (blue) line: CTMC, dashed (blue) line: CTMC-T, thin short-dashed line: SCV, thin black solid line: SDCV, and (green) gray thick solid line: DDCV. (Red) dots correspond to TDSE calculations.

CTMC-T probabilities converge as $\tau \to 0$, which means that, as expected, the inclusion of the tunnel effect is irrelevant in the sudden limit due to the very strong electric field of the HCP. However, the tunnel effect plays an important role for longer pulses where the peak field (Eq. (3)) does not suffice to lower the potential barrier to allow over-the-barrier ionization. As it can be seen in Figure 1, for long pulses the ionization probabilities calculated within the CTMC-T method are considerably higher than those obtained with the CTMC method. There is a critical pulse duration τ_c at which the two curves split. According to case of Figure 1, the classical critical pulse duration is at $\tau_c \simeq 30$ a.u., which corresponds to $F_{0c} \simeq 0.2$ a.u. For $\tau > \tau_c$ over the barrier ionization decreases abruptly and tunneling becomes important, rather the exclusive mechanism of ionization. In this regime of the parameters, the electron completes several orbits around the nucleus during its interaction with the HCP and eventually will be emitted to the continuum through tunneling.

For the momentum transfer $\Delta p = 1$ a.u., in the sudden limit the quantum ionization probability is 44.6%, while the classical one is 50%. According to Figure 2, the classical critical duration at which CTMC and CTMC-T start to run separately is $\tau_c \simeq 8$ a.u., which corresponds to $F_{0c} \simeq 0.4$ a.u. In this case, CTMC-T underestimates the numerical TDSE results for $\tau > \tau_c$ due to the high variation of the envelope of the electric field as a function of interaction time, in combination with the limited number of orbits that the electron occurs around the nucleus. On the other hand, the DDCV reproduces the TDSE calculations very well in the entire range of τ. We note that however SDCV underestimates the TDSE ionization probability for $\tau \gtrsim 10$ a.u. In this case it does not show the anomalous behavior observed before in Figure 1. The agreement between SDCV and CTMC-T in Figure 2 is only circumstantial. The fact that F_{0c} depends on the value of Δp evidences the non-stationary (dynamical) aspect of the ionization process.

Figure 3 shows the total ionization probability as a function of the pulse duration for a lower momentum transfer $\Delta p = 0.5$ a.u. According to Figure 3, for weak momentum transfers both the SDCV and DDCV reproduce the TDSE results reasonably well. More particularly, whereas the SDCV underestimates the TDSE ionization probability, the DDCV overestimates it slightly in the long pulse regime, i.e., $\tau \gtrsim 10$ a.u. On the contrary, CTMC and CTMC-T approaches predict extremely small ionization probabilities, especially for long pulses, where they underestimate considerably the TDSE results. But also for short pulses classical results do not provide proper values of the total ionization probability (see inset of Fig. 3). For pulse durations $\tau > \tau_c \simeq 3$ a.u., tunneling ionization becomes important in the quasiclassical approach but its contribution does not suffice to reproduce the quantum results. It is well known that in the case of weak pulses (dipole or perturbative regime), classical dynamics underestimates the atomic ionization yield [28–31,46]. This effect is referred in the literature as classical suppression [30,31].

3.2 Energy distribution

Figure 4 shows the electron energy distributions for pulses of kick strength $\Delta p = 2.5$ a.u. and different durations. According to Figure 4a, for $\tau = 1$ a.u. the SDCV differs from the TDSE at low electron energies overestimating the near threshold electron yield. This anomalous behavior is overcome by the more elaborated DDCV, which reproduces perfectly the TDSE energy distribution for these field parameters. In the sudden limit quantum-classical correspondence is observed not only in the total ionization yield but also in the energy distribution [28,29], as shown in Figure 4a. However, due to the nonzero temporal width

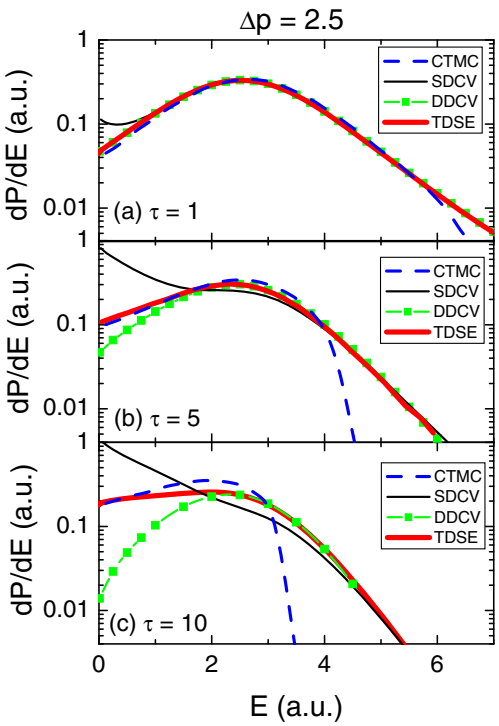

Fig. 4. (Color online) Electron energy distribution after a pulse of momentum transfer $\Delta p = 2.5$ a.u. and duration (a) $\tau = 1$ a.u., (b) $\tau = 5$ a.u., and (c) $\tau = 10$ a.u. (Blue) dashed line: CTMC, thin black solid line: SDCV, (green) squared line: DDCV, and (red) thick solid line: TDSE. For this momentum transfer the CTMC-T result is indistinguishable from the CTMC one.

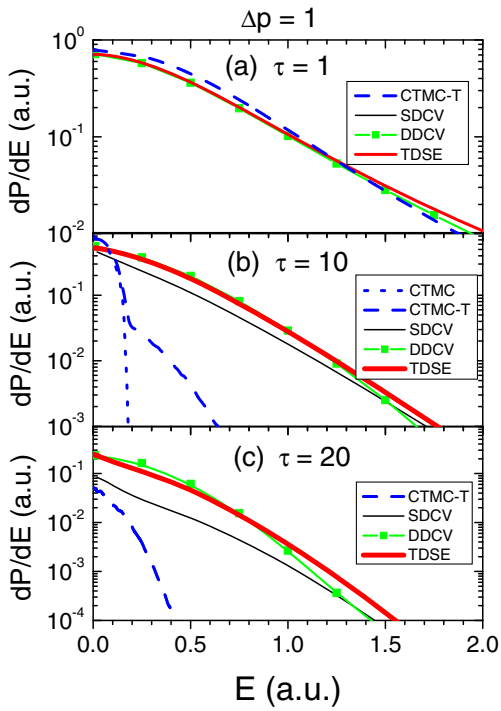

Fig. 5. (Color online) Electron energy distribution after a pulse of momentum transfer $\Delta p = 1$ a.u. and duration (a) $\tau = 1$ a.u., (b) $\tau = 10$ a.u., and (c) $\tau = 20$ a.u. (Blue) dashed line: CTMC, thin black solid line: SDCV, (green) squared line: DDCV, and (red) thick solid line: TDSE. CTMC-T result coincides with CTMC in (a). In (c) CTMC is negligible.

of the HCP, the classical energy distribution departs from the quantum one at high energies, i.e., $E \gtrsim 6$ a.u. The breakdown of the quantum-classical correspondence behavior becomes more pronounced as the duration of the pulse is increased.

As the pulse duration is increased ($\tau = 5$ a.u.), the SDCV behaves properly in the intermediate and high energy regions but fails in the low energy region (see Fig. 4b). The near-threshold anomalous behavior, which is stressed for long pulses, is responsible for the total ionization probability to be higher than one for pulses with intermediate durations in Figure 1. DDCV fixes this problem but underestimates the TDSE energy distribution near the threshold. In addition, the agreement between CTMC and TDSE results deteriorates exhibiting an abrupt decay of the classical curve at $E \gtrsim 4$ a.u.

In Figure 4c we can see that for $\tau = 10$ a.u. both quantum approximations follow the TDSE energy distribution at high energies, but they fail in the low energy region. Whereas SDCV overestimates the TDSE energy distribution near the threshold by an order of magnitude, DDCV underestimates it in the same way. Nevertheless, in the intermediate region DDCV exhibits a substantial improvement with respect to SDCV. Additionally, the CTMC decreases steeply for energies higher than $E \simeq 3$ a.u. but behaves properly just near threshold. In the energy region $1 \lesssim E \lesssim 3$ a.u., CTMC overestimates the numerical TDSE energy distribution compensating the underestimation in the high energy region $E \gtrsim 3$ a.u., providing, in this way, an appropriate total ionization probability as observed in Figure 1.

The value $\Delta p = 1$ corresponds to the intermediate momentum transfer region where classical methods start to fail for short pulses. In both Figures 5b and 5c, whereas the DDCV provides a very good agreement compared to the TDSE results, SDCV underestimates the numerical TDSE energy distribution for a kick strength of $\Delta p = 1$ a.u. On the other hand, for the very short pulse of Figure 5a with $\tau = 1$, all quantum calculations agree. In this case, all classical and quantum approximations agree very well with the TDSE energy distribution showing that quantum-classical correspondence is valid in the sudden limit [28,29]. However, CTMC-T (with the same outcome of CTMC) is slightly higher than the quantum energy distributions, as also observed in the total ionization probability of Figure 2. This behavior was also found for kicks of strength in the range $0.6 \lesssim \Delta p \lesssim 2$ a.u. [46]. The situation dramatically deteriorates for longer pulses ($\tau \geq 10$ a.u.), where the classical approach is unable to reproduce the ionization probabilities (see Figs. 5b and 5c). Even if tunneling is incorporated, CTMC-T underestimates largely the quantum energy distribution almost in the entire energy range.

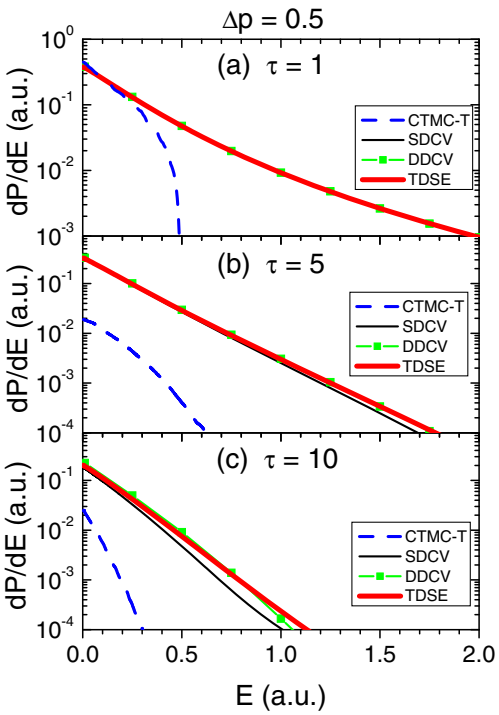

Fig. 6. (Color online) Electron energy distribution after a pulse of momentum transfer $\Delta p = 0.5$ a.u. and duration (a) $\tau = 1$ a.u., (b) $\tau = 5$ a.u., and (c) $\tau = 10$ a.u. (Blue) dashed line: CTMC, thin black solid line: SDCV, (green) squared line: DDCV, and (red) thick solid line: TDSE. CTMC-T result coincides with CTMC in (a). In (b) and (c) CTMC is negligible.

For a kick of $\Delta p = 0.5$ a.u., all quantum approximations studied here reproduce the numerical TDSE values, except for $\tau = 10$ a.u., where SDCV departs slightly from TDSE energy distribution by defect (see Fig. 6c). As mentioned before, the accuracy of the time-dependent distorted wave theories is a direct result of their perturbative nature. In turn, DDCV reproduces the TDSE energy distribution accurately for all the pulse durations. The agreement of the quantum and classical approaches in the sudden limit takes place for high kick strengths [28,29] and deteriorates as Δp decreases. In Figure 6a the CTMC-T results follow the TDSE energy distribution near the threshold but departs from the TDSE curve at $E \simeq 0.3$ a.u. In addition, classical suppression starts to be evident with increasing pulse durations (Figs. 6b and 6c).

4 Conclusions

We conclude that the region of validity of the different quantum and classical approximations studied in this paper depends on the kick strength Δp and the pulse duration τ. The CTMC-T method is able to reproduce the quantum ionization probabilities for large Δp values, even for long pulse durations. For small Δp values quantum approaches are preferable compared to the quasi-classical one, as we depart from the sudden limit. It is in the intermediate limit, i.e., $\Delta p \approx 1$, where known quantum and classical approximations fail. Precisely in this region, DDCV becomes a better alternative than the SDCV, although a deficiency arises at small electron ejection energy for high values of Δp. Summarizing, our DDCV presents a reliable approximation where the CTMC and CTMC-T fails.

This work was carried out with financial support of CONICET, UBACyT X147, and ANPCyT PICT 2006-00772 of Argentina, the Argentine-Hungarian collaboration HU/08/02, the CNCSIS-UEFISCSU proj. No. PNII-IDEI 539/2007, the Hungarian National Office for Research and Technology and the Hungarian Scientific Research Found OTKA (K72172). SB and KT were also partially supported by the European COST Action CM0702.

References

1. J.J. Mestayer et al., Phys. Rev. Lett. **100**, 243004 (2008)
2. D.G. Arbó, C.O. Reinhold, J. Burgdörfer, A.K. Pattanayak, C.L. Stokely, W. Zhao, J.C. Lancaster, F.B. Dunning, Phys. Rev. A **67**, 063401 (2003)
3. F.H.M. Faisal, Schlegel, J. Phys. B **38**, L223 (2005)
4. L.V. Keldysh, Zh. Eksp. Teor. Fiz. **47**, 1945 (1964); Sov. Phys. JETP **20**, 1307 (1965)
5. F.H.M. Faisal, J. Phys. B **6**, L89 (1973)
6. H.R. Reiss, Phys. Rev. A **22**, 1786 (1980)
7. D.B. Milosevic, G.G. Paulus, D. Bauer, W. Becker, J. Phys. B **39**, R203 (2006)
8. D.B. Milosevic, D. Bauer, W. Becker, J. Mod. Opt. **53**, 125 (2006)
9. D. Bauer, D.B. Milosevic, W. Becker, J. Mod. Opt. **53**, 135 (2006)
10. S. Borbély, K. Tőkési, L. Nagy, Phys. Rev. A **77**, 033412 (2008)
11. J.Z. Kaminski, A. Jaron, F. Ehlotzky, Phys. Rev. A **53**, 1756 (1996)
12. D.B. Milosevic, F. Ehlotzky, J. Phys. B **31**, 4149 (1998)
13. D.B. Milosevic, F. Ehlotzky, Phys. Rev. A **58**, 3124 (1998)
14. D. Bauer, D.B. Milosevic, W. Becker, Phys. Rev. A **72**, 023415 (2005)
15. D.B. Milosevic, G.G. Paulus, W. Becker, Opt. Express **11**, 1418 (2003)
16. P.A. Macri, J.E. Miraglia, M.S. Gravielle, J. Opt. Soc. Am. B **20**, 1801 (2003)
17. V.D. Rodriguez, E. Cormier, R. Gayet, Phys. Rev. A **69**, 053402 (2004)
18. G. Duchateau, E. Cormier, R. Gayet, Eur. Phys. J. D **11**, 191 (2000)
19. G. Duchateau, E. Cormier, H. Bachau, R. Gayet, Phys. Rev. A **63**, 053411 (2001)
20. D.G. Arbó, J.E. Miraglia, M.S. Gravielle, K. Schiessl, E. Persson, J. Burgdörfer, Phys. Rev. A **77**, 013401 (2008)
21. R.E. Olson, C.O. Reinhold, D.R. Schultz, High-energy ion-atom collisions, in *Proc. IVth Workshop on High-Energy Ion-Atom Collision Processes* (Debrecen, Hungary, 1990), edited by D. Berényi, G. Hock, Lect. Notes Phys. **376**, 69 (1991), and references therein
22. K. Tőkési, G. Hock, Nucl. Instrum. Meth. B **86**, 201 (1994)
23. K. Tőkési, G. Hock, J. Phys. B **29**, 119 (1996)
24. J.S. Cohen, Phys. Rev. A **64**, 043412 (2001)

25. J.S. Cohen, Phys. Rev. A **69**, 033409 (2003)
26. K.I. Dimitriou, D.G. Arbó, S. Yoshida, E. Persson, J. Burgdörfer, Phys. Rev. A **70**, 061401(R) (2004)
27. D.G. Arbó, S. Yoshida, E. Persson, K.I. Dimitriou, J. Burgdörfer, Phys. Rev. Lett. **96**, 143003 (2006)
28. D.G. Arbó, K. Tőkési, J.E. Miraglia, Eur. Phys. J. D **51**, 303 (2009)
29. D.G. Arbó, K. Tőkési, J.E. Miraglia, Nucl. Instrum. Meth. B **267**, 382 (2009)
30. C.O. Reinhold, J. Burgdörfer, J. Phys. B **26**, 3101 (1993)
31. C.O. Reinhold, M. Melles, H. Shao, J. Burgdörfer, J. Phys. B **26**, L659 (1993)
32. D.M. Volkov, Z. Phys. **94**, 250 (1935)
33. R. Abrines, I.C. Percival, Proc. Phys. Soc. **88**, 861 (1966)
34. R.E. Olson, A. Salop, Phys. Rev. A **16**, 531 (1977)
35. E.C. Kemble, Phys. Rev. **48**, 549 (1935)
36. M.S. Child, Molec. Phys. **12**, 401 (1967)
37. J.N.L. Connor, Molec. Phys. **15**, 37 (1968)
38. K.I. Dimitriou, S. Yoshida, J. Burgdörfer, H. Shimada, H. Oyama, Y. Yamazaki, Phys. Rev. A **75**, 0013418 (2007)
39. X.-M. Tong, S.I. Chu, Chem. Phys. **119**, 217 (1997)
40. D.G. Arbó, K.I. Dimitriou, E. Persson, J. Burgdörfer, Phys. Rev. A **78**, 013406 (2008)
41. S. Dionissopoulou, Th. Mercouris, A. Lyras, C.A. Nicolaides, Phys. Rev. A **55**, 4397 (1997)
42. O. Schöller, J.S. Briggs, R.M. Dreizler, J. Phys. B: At. Mol. Phys. **19**, 2505 (1986)
43. A. Messiah, *Quantum Mechanics 1* (North-Holland, New York, 1965)
44. R. Moshammer et al., Phys. Rev. Lett. **79**, 3621 (1997)
45. V.D. Rodriguez, P. Macri, R. Gayet, J. Phys. B **38**, 2775 (2005)
46. D.G. Arbó, C.O. Reinhold, P. Kürpick, S. Yoshida, J. Burgdörfer, Phys. Rev. A **60**, 1091 (1999)